

Vibration and wave processes in view of non-linear deformation of components in aircraft engine hydraulic systems

Dinara F. Gaynutdinova Vladimir Ya. Modorsky Vasiliy Yu. Petrov
grigoriev@ispms.tsc.ru

Abstract

We performed numerical studies of hydroelastic vibration and wave processes which included two approaches: one solving coupled problems in ANSYS CFX software package, and another using national algorithm for solving problems of hydroelasticity stated as a couple. In ANSYS CFX package we obtained results of computational modelling of cavitation effect caused by vibrations of the wall in a closed type (return-flow) pipe filled with fluid. We revealed the dependence between the cavitation parameters and the vibration parameters. We also constructed the domain (range) of influence of amplitudes and frequencies of vibration upon concentration of cavitation bubbles. At the second stage of the studies we developed standardized algorithm for solving problems of dynamic hydroelasticity, worked out the model problem of piston motion of piston in the closed type pipe, and conducted a comparative analysis of numerical and analytical solutions of the model problem.

Introduction

Unpredictable failures in the course of operation of hydraulic automatic equipment of aircraft engines occur increasingly often. To predict them is a difficult and time-consuming task. It is true that failures may be related to the drastic increase of operation noise generated by hydraulic systems of aircraft engines, and therefore it might be suggested that they are brought about by cavitation effects in the pipelines caused by vibrations of the component walls. This paper is concerned with the possibility of modelling the cavitation effect during the operation of hydraulic automatic equipment.

1 Solution of the Problem in ANSYS CFX Software Package

Physical Model

To carry out computing experiments we developed a physical model which proposed a three-dimensional statement. In doing so, we took a pipe as the computation domain, compressible fluid (water) as the actuating medium, and sinusoidally movable

wall as the loading; assumed that the flow was multiphase (consisting of water as carrier phase, and air as carried phase), the process was adiabatic, and the pipe walls were impenetrable and smooth, and accepted standard ke model of turbulence.

Mathematical Model

In accordance with the accepted physical model, we used a mathematical model based on the mass, momentum and energy conservation laws, and implemented within ANSYS CFX reverse engineering system. It reflected the convection-diffusion transfer of components to be mixed and turbulent flow. The set of equations was enclosed by the initial and boundary conditions. [1]

The finite volume method implemented in ANSYS CFX software package was chosen to solve the original set of equations.

Solid Model and Setting of Initial and Boundary Conditions

The computational domain was divided into finite volumes (400,000 cells). Figure 1 shows the solid model and boundary conditions. The following initial conditions were set: $V = 0$ m / s; $P = 0.1$ MPa; $T = 293$ K; $\rho_w = 1000$ kg/m³.

The boundary condition adopted for the walls of chamber was "stiff or rigid wall" when the normal velocity component at the boundary was equal to 0. The boundary condition adopted for the mobile body was movable wall when the normal velocity component at the boundary was set by equation $V = V_0 \sin(\omega t)$, where V – flow or fluid velocity, V_0 – wall velocity amplitude, ω – oscillation frequency, and t – time. [2] - [5]

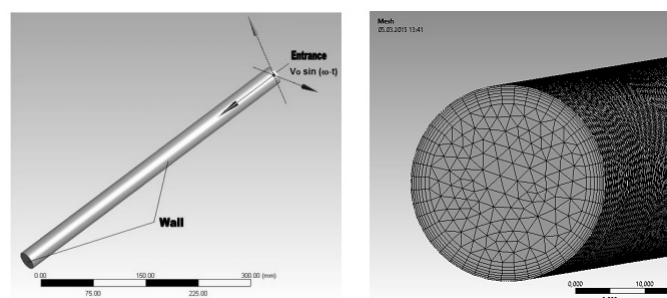


Figure 1: Boundary Conditions and Computational Grid

The time step was set at $5 \cdot 10^{-4}$ sec, and the number of iterations for each calculation did not exceed 2000. Therefore, each of the options was studied on the real-time interval from 0 to 1 sec. The calculation time was 4...5 hours.

Analysis of the Results of Computing Experiments

The plan of computing experiments envisaged that V_0 varied in the range $0.001 \dots 10 \text{m/sec}$ and ω - in the range $500 \dots 4000 \text{ Hz}$. All calculations were made on the basis that the initial pressure within an enclosure was 1 MPa at an initial temperature (T) of 20°C .

In accordance with the plan, different values of carried phase concentration were derived from the results of computing experiments.

According to the calculations based on all options of set boundary conditions, we obtained a certain area of cavitation arising due to vibration at various combinations of frequencies and wall velocity amplitudes. In Fig. 2: x-axis is used to specify the change in the speed of oscillation, y-axis to specify the change in the frequency of oscillation, and z-axis the change in the mass content of carried phase. [6]

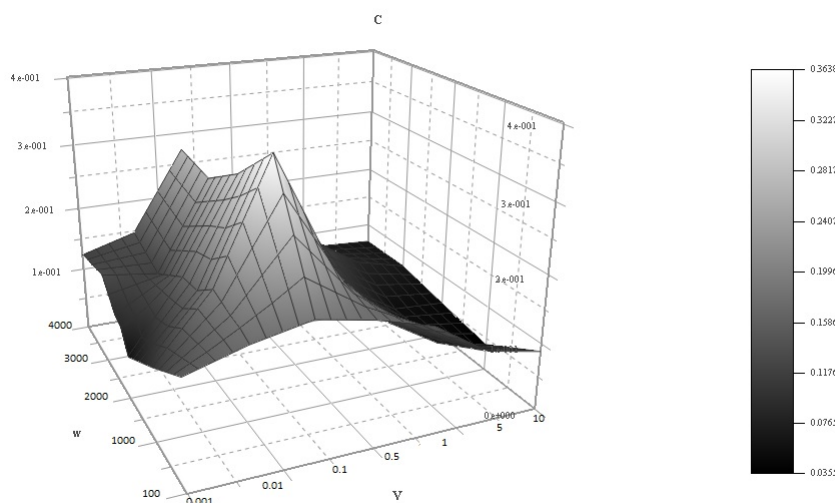


Figure 2: Area of Cavitation Due to Vibration

The analysis of the results revealed a maximum corresponding to the frequency of 2000 Hz . As the frequency of vibration increased or decreased the concentration decreased. The wall velocity amplitude corresponding to the maximum concentration of the carried phase was 0.1 m/sec , and as it increased or decreased the concentration decreased as well.

2 Development and Implementation of Standardized Algorithm Based on the Particle-in-Cell Method

At present, with current sanctions against Russia, this is particularly important to develop national algorithms for solving complex interdisciplinary problems, including hydroelasticity.

Physical Model

We developed the physical model that enabled the processes occurring in structure and in fluid to be stated dynamically in two-dimensions; for that purpose, we assumed that the structure was multilayered and made of elastic material; the fluid was compressible and remained in contact with the movable wall; and the pipe walls were impenetrable, impermeable, not heat conducting and smooth; and took no account of gravity.

Mathematical Model

In accordance with the accepted physical model, we constructed a mathematical model of hydrodynamic process based on the mass, momentum and energy conservation laws, control of compressible fluid state, and initial and boundary conditions recorded with due regard for stiffness of loading system.

Mathematical model of deformable structure also included the mass and momentum conservation laws, and was enclosed by Cauchy equations, generalized Hookes law, and initial and boundary conditions recorded with due regard for stiffness of loading system.

To develop the original system of differential equations we chose one of the methods of finite differences - the particle-in-cell method.

Standardized Algorithm for Solving Problems of Dynamic Hydroelasticity

Based on the chosen method we developed the algorithm which included several stages (Figure 3). The initial stages were designed to solve the hydrodynamic problem, whereas the subsequent stages were meant to estimate parameters of the dynamic stress-strain state (SSS) or tensely deformed condition (TDC) of structure. [7]

First, we described the initial conditions and produced a computational grid in the field of solution for both fluid and structure. Then, we formed the boundary conditions for the fluid with due regard for the loading system, and then focused on three successive stages. At the Eulerian stage we neglected all effects associated with the movement of unit cell (when there was no mass flow through the cell borders), and took into account the effects of material acceleration only through pressures; here we determined intermediate values of the desired flow conditions (characteristics) for a large particle. At the Lagrangian stage we calculated the mass flows crossing the borders of the Eulerian cells. At the final stage, at a new moment we determined the final values of the flow conditions (characteristics) for each cell, and for the entire system on the fixed computational grid. The obtained parameters of hydrodynamic flow were used as the initial data for the subsequent time step and were included in the calculations of the boundary conditions to estimate the dynamic stress-strain state (SSS) or tensely deformed condition (TDC) of structure.

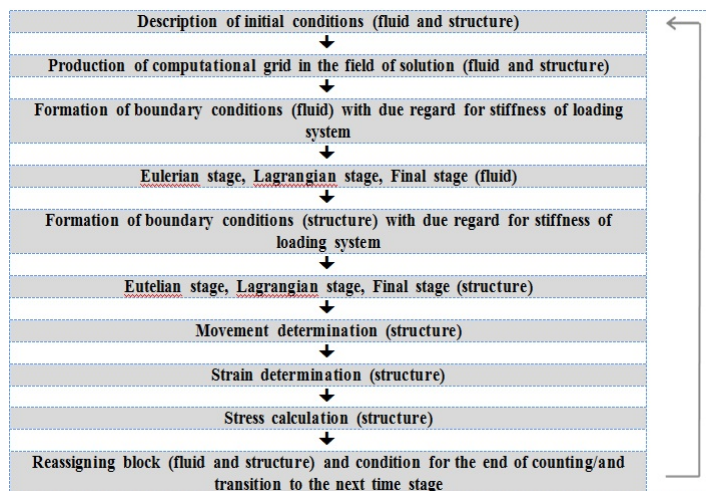


Figure 3: Standardized Algorithm for Solving Problems of Dynamic Hydroelasticity

Further, the same three stages were sequentially performed for the structure. The following stages were new from the viewpoint of traditional approaches to the particle-in-cell method and included algorithms to determine the movements, strains and stresses at each time step. That completed the computing cycle of one time step, and the results of calculation at that time step provided a baseline for the next one.

The use of this standardized algorithm for simultaneous solution of hydrodynamic problem and calculation of parameters of the stress-strain state of the structure is an innovation and makes it possible to study and reveal the physical entity of the occurrence and course of abnormal unpredictable hazardous processes and phenomena in case of the nonlinear interaction in the dynamic system using the united methodological tools. This will allow finding ways to ensure operability of expensive high-tech structures yet at the design stage.

Analysis of the Results of Model Problem Solution

Testing of the proposed algorithm for solving problems of dynamic hydroelasticity was conducted in MARS domestic package for the model problem about the motion of piston in the fluid filled pipe. Design scheme is presented in Figure 4.

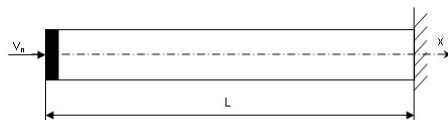


Figure 4: Design Scheme

The following initial conditions were set: $L = 0.5\text{m}$ – the pipe length; $P_{in} = 450 \cdot 10^6\text{Pa}$ – internal fluid pressure; $V = 10\text{m/sec}$ – the speed of piston; $\rho_w = 1000\text{kg/m}^3$ – the liquid density; $K = 5.0$ – fluid adiabatic exponent. In this case,

at this stage the structure is not deformable (strained), but this may be considered in future.

Upon starting, the wave of compression will move ahead of the piston at a speed of N_1 in a medium at rest (fluid at rest). Once it reaches the wall, the direct wave will reflect from the wall, and the reflected wave will propagate at a speed of N_3 in the direction opposite to that of the moving fluid (Figure 5.). [8]



Figure 5: Direct and Reflected Waves

Results of the solution of model problem for the direct wave are given in Figure 6. The figure shows that the front of direct wave has run halfway along the pipe length. Downstream the wave front there are oscillations caused by numerical effects.

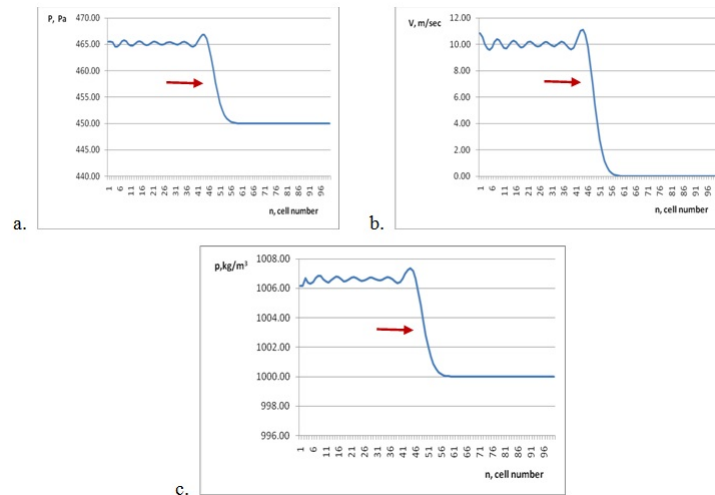


Figure 6: Change in Hydrodynamic Parameters along the pipe length, at $t = 0.16 \cdot 10^{-3} \text{sec}$, a. – pressure b. – speed c. – density

Subsequently, after the reflection these effects disappear. Results of the solution of model problem of the reflected wave are shown in Figure 7.

To verify the obtained numerical solutions analytical calculations for this model problem were made with the use of known analytical dependences.

Table 1 gives the results of comparison between numerical and analytical solutions in the following parameters: P_1 , ρ_1 – pressure and density of the direct wave, respectively; X_1 – displacement of the front of direct shock wave from the original position; N_1 – speed of the front of direct wave; P_3 , ρ_3 – pressure and density of the reflected wave, respectively; X_3 – displacement of the front of reflected wave from the original position; N_3 – speed of the front of reflected wave.

The comparative analysis of numerical and analytical solutions has shown that the results of solutions agree very closely. There is a "smearing" of the shock wave front associated with the schematic viscosity.

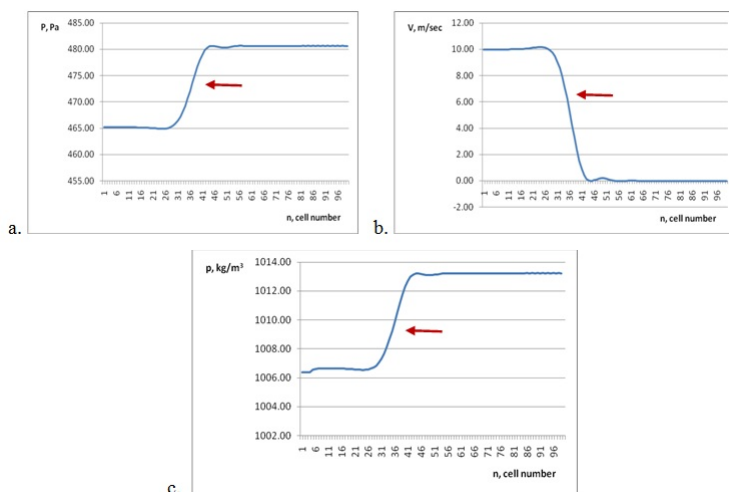


Figure 7: Change in Hydrodynamic Parameters along the pipe length, at $t = 0.57 \cdot 10^{-3}$ sec, a. – pressure b. – speed c. – density

Table 1: Comparison between Numerical and Analytical Solutions

| Controlled Parameters | Results of Numerical Solution | Results of Analytical Solution |
|-------------------------|-------------------------------|--------------------------------|
| P_1, Pa | $465 \cdot 10^6$ | $465 \cdot 10^6$ |
| $\rho_1, \text{kg/m}^3$ | 1006,6 | 1006,6 |
| X_1, m | 0,24 | 0,24 |
| $N_1, \text{m/sec}$ | 1515 | 1515 |
| P_3, Pa | $480,6 \cdot 10^6$ | $480,6 \cdot 10^6$ |
| $\rho_3, \text{kg/m}^3$ | 1013,3 | 1013,3 |
| X_3, m | 0,36 | 0,36 |
| $N_3, \text{m/sec}$ | 1525 | 1525 |

Conclusions

1. We have carried out the studies using two approaches: on the basis of the solution of the coupled problem in ANSYS CFX commercial package and MARS domestic package, and solved hydroelasticity problems stated as a couple.

2. We have constructed physical and mathematical models for computing experiment and performed numerical computations. We have discovered and constructed the area of cavitation brought about by vibration, and have revealed that the cavitation effect was maximized at certain combinations of amplitudes and frequencies of oscillations.

3. To develop national algorithm for solving coupled problems of dynamic hydroelasticity we have constructed physical and mathematical models, and have developed standardized algorithm. We have solved the model problem of dynamic hydroelasticity stated in one dimension. We have made analytical calculations and comparative analysis with the numerical solution. It has shown that their results

agree very closely.

Acknowledgements

The work is carried out with the support of the Russian Foundation for Basic Research, Grant RFFI No. 14 – 07 – 96003 – r_ural.a.

References

- [1] Reverse Engineering System ANSYS CFX-Solver Theory Guide. ANSYS CFX.
- [2] The solution of engineering problems on high performance computing complex of the Perm National Research Polytechnic University: monograph edited by V.Ya. Modorsky - Perm: Publishing of the Perm National Research Polytechnic University, 2014. – 314 pp.
- [3] A.V. Kozlova, V.Ya. Modorsky. Numerical modeling of the cavitation effects in a closed type pipe with a movable wall. Scientific and Technical Bulletin of Povolzhye. No. 2 2013 – Kazan: Scientific and Technical Bulletin of Povolzhye, 2013. – pp. 132-135.
- [4] D.F. Gaynutdinova, A.V. Kozlova, V.Ya. Modorsky, E.V. Mekhanoshina. Numerical modeling of the cavitation effects caused by vibration. Scientific and Technical Bulletin of Povolzhye. No. 6 2013 – Kazan: Scientific and Technical Bulletin of Povolzhye, 2013. – pp. 219-223.
- [5] E.V. Mekhanoshina, V.Ya. Modorsky, A.V. Kozlova, D.F. Gaynutdinova, Study of the influence of vibration and pressure on cavitation. Scientific and Technical Bulletin of Povolzhye. No. 6 2013 – Kazan: Scientific and Technical Bulletin of Povolzhye, 2013. – pp. 364-368.
- [6] Gaynutdinova D.F., Modorsky V.Ya., Kozlova A.V. Computing modeling of the area of cavitation caused by vibration. Scientific and Technical Bulletin of Povolzhye. No. 6 2014 – Kazan: Scientific and Technical Bulletin of Povolzhye, 2014. – pp. 127-129.
- [7] Modorsky V.Ya., Sokolkin Yu.V. Gas Elastic Processes in Power Plants. – M.: Nauka, 2007 – 176 pp.
- [8] I.P. Ginzburg Aerogas dynamics. – M.: Vysshaya Schkola, 1966 – 404 pp.

Dinara F. Gaynutdinova, pr. Komsomolsky, 29, Perm, Russian Federation
Vladimir Ya. Modorsky, pr. Komsomolsky, 29, Perm, Russian Federation
Vasilij Yu. Petrov, pr. Komsomolsky, 29, Perm, Russian Federation